Mechanisms Governing the Endosomal Membrane Recruitment of the Core Retromer in Arabidopsis

Enric Zelazny, Pierre Chambrier, Annick Berne-Dedieu, Mikael Pourcher, Martina Santambrogio, Nelcy Thazar, Anne-Marie Thierry, Isabelle Fobis-Loisy, Christine Miege, Yvon Jaillais, et al.

THE JOURNAL OF BIOLOGICAL CHEMISTRY VOL. 288, NO. 13, pp. 8815–8825, March 29, 2013

Mechanisms Governing the Endosomal Membrane Recruitment of the Core Retromer in *Arabidopsis*[*] [S]

Received for publication, November 28, 2012, and in revised form, January 18, 2013 Published, JBC Papers in Press, January 29, 2013, DOI 10.1074/jbc.M112.440503

Enric Zelazny[1], Martina Santambrogio[1], Mikael Pourcher, Pierre Chambrier, Annick Berne-Dedieu, Isabelle Fobis-Loisy, Christine Miège, Yvon Jaillais, and Thierry Gaude[2]

From the CNRS, F-69342 Lyon, France, the Institut National de la Recherche Agronomique, F-69364 Lyon, France, the Ecole Normale Supérieure de Lyon, F-69342 Lyon, France, the Université Lyon 1, F-69622 Villeurbanne, France, and the Unité Mixte de Service Biosciences Gerland, F-69366 Lyon, France

Background: The retromer is an endosome-localized complex involved in intracellular trafficking that remains understudied in plants.
Results: *Arabidopsis* vacuolar protein sorting (VPS)35 plays a key role in the membrane recruitment of the retromer and interacts with a Rab7 homolog, RABG3f.
Conclusion: We propose a model in which plant retromer membrane recruitment involves RABG3f/VPS35 interaction.
Significance: The plant retromer exhibits original mechanistic features compared with other organisms.

The retromer complex localizes to endosomal membranes and is involved in protein trafficking. In mammals, it is composed of a dimer of sorting nexins and of the core retromer consisting of vacuolar protein sorting (VPS)26, VPS29, and VPS35. Although homologs of these proteins have been identified in plants, how the plant retromer functions remains elusive. To better understand the role of VPS components in the assembly and function of the core retromer, we characterize here *Arabidopsis vps26*-null mutants. We show that impaired *VPS26* function has a dramatic effect on VPS35 levels and causes severe phenotypic defects similar to those observed in *vps29*-null mutants. This implies that functions of plant VPS26, VPS29, and VPS35 are tightly linked. Then, by combining live-cell imaging with immunochemical and genetic approaches, we report that VPS35 alone is able to bind to endosomal membranes and plays an essential role in VPS26 and VPS29 membrane recruitment. We also show that the *Arabidopsis* Rab7 homolog RABG3f participates in the recruitment of the core retromer to the endosomal membrane by interacting with VPS35. Altogether our data provide original information on the molecular interactions that mediate assembly of the core retromer in plants.

The retromer complex is a coat complex localized to the cytosolic face of endosomes and involved in intracellular sorting of specific transmembrane proteins, known as cargoes (1). In mammals, the retromer is made up of five proteins that associate to form two distinct subcomplexes. The first is composed of a dimer of sorting nexins (SNXs),[3] including SNX1, SNX2, SNX5, and SNX6, which associate with the membrane of endosomes and lead to their tubulation (2–4). The second is known as the core retromer and consists of a trimer of vacuolar protein sorting (VPS) 26, VPS29, and VPS35 (1). Because VPS35 binds directly to the cytosolic tail of cargo proteins, the core retromer is considered as the cargo loading complex (5–9). The mechanism of recruitment of the retromer complex to the endosomal membrane has been the object of numerous studies. SNX proteins possess membrane binding properties that allow them to associate with the endosomal membrane and then to recruit the core retromer at the surface of endosomes (10). In addition, VPS26 was suggested to be important in recruiting the VPS subcomplex to membranes in yeast and mammalian cells (11), although other studies provided evidence for a central role of VPS35 in membrane association (12, 13). Besides, two small guanosine triphosphatases (GTPases), Rab5 and Rab7, were shown to act sequentially to control the recruitment of the human retromer complex to endosomes (14, 15).

Components of the retromer complex are conserved in *Arabidopsis thaliana* (16, 17). There are three genes encoding VPS35 isoforms (*VPS35a*, *VPS35b*, and *VPS35c*), two encoding VPS26 isoforms (*VPS26a* and *VPS26b*), one gene coding for VPS29, and three SNX genes, designated *SNX1*, *SNX2a*, and *SNX2b* (17). A dual localization, free in the cytosol or associated with the membrane of endosomes, was reported for plant retromer components (16, 18–20).

Early studies on the plant retromer complex relying on the analysis of null mutants of the single *VPS29* gene showed that VPS29 is required for endosome homeostasis, protein trafficking, and recycling of the auxin efflux carrier PIN1 (16, 21). Similar phenotypes were observed in various *vps35* combinatory mutants, arguing in favor of VPS35 isoforms acting together and in association with VPS29 (19). To date, null mutants of

* This work was supported by the Agence Nationale de la Recherche BLANC RETROMER Project Grant ANR-08-BLAN-0142.
[S] This article contains supplemental Figs. 1–4, Table 1, and Experimental Procedures.
[1] These authors contributed equally to this work.
[2] To whom correspondence should be addressed: ENS Lyon, Plant Reproduction and Development Laboratory, 46 allée d'Italie, 69364 Lyon Cedex 07, France. Tel.: 334-72-72-86-09; Fax: 334-72-72-86-00; E-mail: thierry.gaude@ens-lyon.fr.

[3] The abbreviations used are: SNX, sorting nexin; BiFC, bimolecular fluorescence complementation; FBPase, fructose-1,6-bisphosphatase; IP, immunoprecipitation; VHA-a1, vacuolar H^+-ATPase-a1; VPS, vacuolar protein sorting.

VPS26 have never been described. Here, we report that double null mutants for *VPS26a* and *VPS26b* present developmental defects similar to *vps29* loss-of-function mutants, suggesting that plant VPS26, VPS29, and VPS35 function as a complex in the same developmental pathways.

Because the process of assembly of a multiprotein complex is important to understand its function and regulation, we investigated how the plant retromer components are targeted to the endosomal membrane and physically associate to form a functional complex. Recently, we reported that, contrary to the mammalian retromer, SNXs are dispensable for membrane binding and function of the retromer complex in plants. We found that the core retromer can work independently of SNXs in protein trafficking and plant development, indicating distinct functions for these subcomplexes in plant cells (20). Here, we demonstrate that the formation of the core retromer complex can occur in the cytosol and that domains of VPS35, known to be important for yeast and mammalian retromer assembly, play similar roles in *Arabidopsis*. Moreover, we reveal a distinct mode of assembly of the core retromer in plant cells compared with other organisms, because VPS35 does not require VPS26 and VPS29 proteins to be anchored to membranes. In addition, we show that VPS35 interacts with an *Arabidopsis* Rab7 homolog, RABG3f, which might therefore participate in the recruitment of the VPS subcomplex to the endosomal membrane. Altogether, our data reveal that although some mechanisms are conserved, the plant retromer displays specific mechanistic features compared with its yeast and mammalian counterpart.

EXPERIMENTAL PROCEDURES

Plant Material and Growth Conditions—The *A. thaliana* Columbia 0 (Col-0) accession was used as a wild type (WT). The *vps26a-1* (GABI 311E08), *vps26a-2* (GABI 076F06), *vps26b-1* (SALK 142592) T-DNA insertion lines were obtained from Bernd Weisshaar (Max Planck Institute for Plant Breeding Research; Cologne, Germany) and from the SALK Institute (22), respectively. We generated two double mutants with these lines: *vps26a-1 vps26b-1* and *vps26a-2 vps26b-1*. *snx1-2 snx2a-2 snx2b-1* (20), *vps29-1*, *vps29-3*, *vps29-4* (16, 21) and *vps35a-1 vps35c-1* (19) were described previously. p35S: gVPS29-GFP (16), p35S:GFP-RabF2b (23), pVHA-a1:VHA-a1-GFP (24), YFP-RABG3f (25), and Myr-2× m-Citrine (26) lines were described previously. Plants were grown in soil with long daylight (16 h of light/8 h of dark) at 21 °C and 70% humidity.

Plasmid Constructions and Site-directed Mutagenesis of VPS35a— 615 bp upstream of the 5′-UTR of *VPS35a* were amplified by PCR with the primer pair B4-VPS35aPro/B1rVPS35aPro and cloned in the pDONRP4-P1R vector (Invitrogen). The genomic DNA corresponding to *VPS35a* (from 5′-UTR to the last codon) was amplified by PCR with the primer pair VPS35a-TOPO/TOPO-VPS35a-STOP and cloned in the pENTR/D-TOPO vector (Invitrogen). *pVPS35a:gVPS35a* DNA fragments were cloned in-frame with a GFPS65 (27) in a pH7m34GW vector (28). Transgenic plants were generated as described in Ref. 23.

Site-directed mutagenesis of *VPS35a* was performed independently on Arg-104 and Leu-105 residues to replace them with Trp-104 and Pro-105, respectively. Mutations were created by PCR with specific primers designed by the Stratagene QuikChange primer Design Program on the cDNA sequence of *VPS35a* in the pDONRZeo vector (Invitrogen). PCR was made with the Phusion Taq (Ozyme, France). PCR products were digested by the enzyme DpnI following the manufacturer's instructions. The remaining DNAs were transformed in *Escherichia coli* DH5α. To obtain *VPS35a-ΔC-END*, we cloned the *VPS35a* cDNA from ATG to bp 1938 in the pDONRZeo vector. The following primer pairs were used: 35a-R104W-F/35a-R104W-R, 35a-L105P-F/35a-L105P-R, and 35a-ΔC-END-F/35a-ΔC-END-R.

For transient expression in tobacco leaves, *VPS35a* mutated/truncated forms were cloned in pK7WGF2 vector (28, 29) containing the *35S* promoter and allowing N-terminal fusion with the GFP. *RABG3f* cDNA was amplified with RABG3f.F and RABG3f.R primers and cloned in the pDONRZeo plasmid before recombination in the pK7WGF2 vector to allow N-terminal fusion with the GFP. To generate the *35S:mCherry-VPS35a* fusion, *VPS35a* cDNA was amplified with attB2R. VPS35a and attB3.VPS35a primers and cloned in pDONRP2R-P3 (Invitrogen) before recombination with pDONRP4-P1R-p35S and pDONR221-mCherry in pH7m34GW vector (28).

For bimolecular fluorescence complementation (BiFC) analysis, cDNAs of *VPS35a*, *VPS26a*, and *VPS29* were cloned in pBIFP vectors to produce both N-terminal and C-terminal fusions to either the N-terminal half (NE) or the C-terminal half (CE) of the yellow fluorescent protein (YFP) (30). The mutated/truncated *VPS35a* cDNAs were cloned in the pBIFC2 and pBIFC3 vectors to produce N-terminal fusions with NE-YFP and CE-YFP, respectively.

For yeast two-hybrid assays, *AD-VPS26a*, *AD-VPS29*, *BD-VPS35a* constructs have been described previously (16). *VPS26b* cDNA was amplified with the primer pair 26b-B1-Kozak/26b-B2+STOP and cloned in the pDONRZeo vector (Invitrogen). Then, pDONRZeo-VPS26b was recombined in the pPC86-CYH2^s vector for fusion with the AD of Gal4. VPS35a-R104W, VPS35a-L105P, and VPS35a-ΔC-END were cloned in the pPC97 vector for fusion with the BD of Gal4. pDONRZeo-RABG3f was recombined in pACT2-GW vector to fuse RABG3f to the AD of Gal4. The list of primers used is in supplemental Table 1.

Root Phenotype and Statistical Analysis—For root growth analysis, seedlings were grown vertically on Murashige and Skoog (MS) medium containing 1% sucrose in Petri dishes for the indicated period of time. Root length was measured using the software ImageJ. All of the experiments were repeated at least three times (15 seedlings/experiment) independently. p values indicated for the primary root length measurements were obtained with a two-sided Student's test assuming unequal variances. Calculations were performed with Excel 2007.

Analysis of Seed Storage Proteins—Total proteins were extracted from 100 dry seeds, and 12 μg of proteins was analyzed by SDS-PAGE. Proteins were either stained by Coomassie Blue coloration or detected by Western blotting using anti-12S-globulin (1:10,000 dilution (31)) and anti-2S-albumins (1:1000 dilution (31)) antibodies, as described previously (20).

Yeast Two-hybrid Assays—These experiments were performed as described previously (16).

Cell Fractionation and Western Blotting—100 mg of ~1-month-old plantlets grown on MS medium supplied with 1% sucrose, or 100 mg of tobacco leaves collected 3 days after infiltration were ground in 1 ml of microsomal extraction buffer (500 mM sucrose, 50 mM Hepes, pH 7.4, 1 mM DTT, 5 mM EDTA, 5 mM EGTA, and Complete Mini EDTA-free Protease Inhibitor mixture tablets (Roche Applied Science)). Extracts were centrifuged at 13,000 × *g* for 20 min at 4 °C to eliminate cell debris. Supernatants were centrifuged again at 13,000 × *g* for 10 min at 4 °C. Supernatants were then subjected to ultracentrifugation at 100,000 × *g* for 90 min at 4 °C. Supernatants (cytosolic fractions) and pellets (microsomal fractions) were analyzed by Western blotting using 10 μg of proteins. The following antibodies were used: anti-GFP (1:1000 dilution; Roche Applied Science), anti-VPS29 (1:1000 dilution (16)), anti-VPS35a (1:1000 dilution (21)), anti-α-tubulin (1:1000 dilution; Sigma Aldrich), anti-H^+-ATPase (1:10,000 dilution (32)), and anti-cytosolic fructose-1,6-bisphosphatase (FBPase) (1:30,000 dilution; Agrisera) antibodies. H^+-ATPase and FBPase proteins were used as markers of membrane and cytosolic fractions, respectively.

Co-immunoprecipitation—After cell fractionation, pellets were resuspended in 1 ml of lysis buffer (Kit Miltenyi Biotech), whereas supernatants (500 μl/sample) were diluted with 500 μl of lysis buffer. Protein extracts were subjected to co-immunoprecipitation (Co-IP) using the anti-GFP antibody as described previously (16). Eluted proteins were analyzed by Western blotting as described above.

BiFC Analyses and Tobacco Transient Transformation—The BiFC assays and the infiltration of tobacco leaves were performed as previously described (20).

Confocal Microscopy—*A. thaliana* roots of 7-day-old seedlings grown on MS medium or pieces of infiltrated tobacco leaves were analyzed with a LSM510 or LSM710 Laser-scanning Confocal Microscope (Zeiss, Jena, Germany) as described (23). Each experiment was repeated at least three times independently.

Accession Numbers—Sequence data from this article can be found in the *Arabidopsis* Genome Initiative database under the following accession numbers: VPS26a (At5g53530), VPS26b (At4g27690), VPS29 (At3g47810), VPS35a (At2g17790), VPS35b (At1g75850), VPS35c (At3g51310), RABF2b (At4g19640), and RABG3f (At3g18820).

Genotyping of vps26 Mutants and RT-PCR—Genotyping of *vps26* mutants and RT-PCR are described under supplemental Experimental Procedures.

RESULTS

Arabidopsis VPS29, VPS35 and VPS26 Act in Concert in the Same Pathways—If the plant retromer functions only under the form of a complex, we expect components of the retromer to be involved in the same physiological processes and hence to be expressed in the same tissues, organs, or during the same stages of plant development. To check whether the expression patterns of the core retromer encoding genes overlap, we performed an *in silico* analysis using Genevestigator. We found that all *VPS* retromer genes were simultaneously expressed (supplemental Fig. 1). Surprisingly, the single *VPS29* gene revealed to be always the most abundantly expressed, with, in some cases, levels of transcripts up to four times higher than any of the other core retromer genes.

Although mutants impaired in *VPS29* or *VPS35* functions have been described, so far, null mutants of *VPS26* have never been reported in *Arabidopsis*. Therefore, we decided to uncover the function of VPS26 proteins and to determine whether both isoforms act together with or independently from VPS29 and VPS35, by analyzing T-DNA insertion-null mutants of *VPS26a* (*vps26a-1* and *vps26a-2*) and of *VPS26b* (*vps26b-1*) (supplemental Fig. 2). *vps26a* and *vps26b* single mutants were indistinguishable from wild-type plants, suggesting that these two genes are redundant (data not shown). We generated the following double mutants, *vps26a-1 vps26b-1* and *vps26a-2 vps26b-1*, which both displayed a strong alteration in seedling growth and development that was similar to that of *vps29*-null mutants (16). Indeed, cotyledons were affected, showing abnormal shape and positioning (Fig. 1*A*), rosettes were reduced in size, and adult *vps26a vps26b* plants were dwarf compared with wild-type plants (Fig. 1*B*). Like *vps29* mutants, *vps26a vps26b* seedlings exhibited strong defects in primary root growth, which revealed to be even stronger than in *vps29* mutants (Fig. 1*C*).

Maturation of the major seed storage proteins of *Arabidopsis*, the 2S-albumin and 12S-globulin, was previously shown to be altered in retromer mutants, with part of these proteins being secreted out of the cell. This misrouting is responsible for the abnormally high levels of the precursors of 2S-albumin and 12S-globulin that accumulate in *vps29* single mutant and *vps35a vps35c* double mutants (19, 21). Thus, we investigated whether also in *vps26a vps26b* mutants the maturation of seed storage proteins was affected. We compared the storage protein patterns of wild-type (WT) and *vps26* mutant dry seeds by immunoblot analysis using specific anti-12S-globulin and anti-2S-albumin antibodies. We found that *vps26a vps26b* double mutant seeds showed accumulation of 12S-globulin (p12S) and 2S-albumin (p2S) precursors accompanied by a strong reduction in the level of mature 12S-globulin (12S) (Fig. 1, *D* and *E*). Altogether, these results reveal that the concomitant loss of function of both VPS26a and VPS26b recapitulates the *vps29* phenotypes and hence, indicate that the VPS26 isoforms and VPS29 function together in mediating the same physiological processes. Our genetic analysis, combined with previous genetic and biochemical studies (16, 19, 21), allows us to assume that the products of *VPS29*, *VPS35*, and *VPS26* genes act together in the form of a mutiprotein complex to accomplish common cellular and physiological functions in plants.

Core Retromer Stability and Recruitment to Membranes in Plants—We previously showed that the SNX subcomplex is dispensable for the membrane localization of the plant core retromer (20). We therefore tested the possibility of an autonomous membrane recruitment of the VPS subcomplex. To study the core retromer assembly and determine whether one of the three VPS proteins could recruit the other two to membranes, we investigated the interaction between VPS35/VPS26 and VPS35/VPS29 proteins by BiFC assays in *Nicotiana benthamiana* epidermal leaf cells. Although a complex between

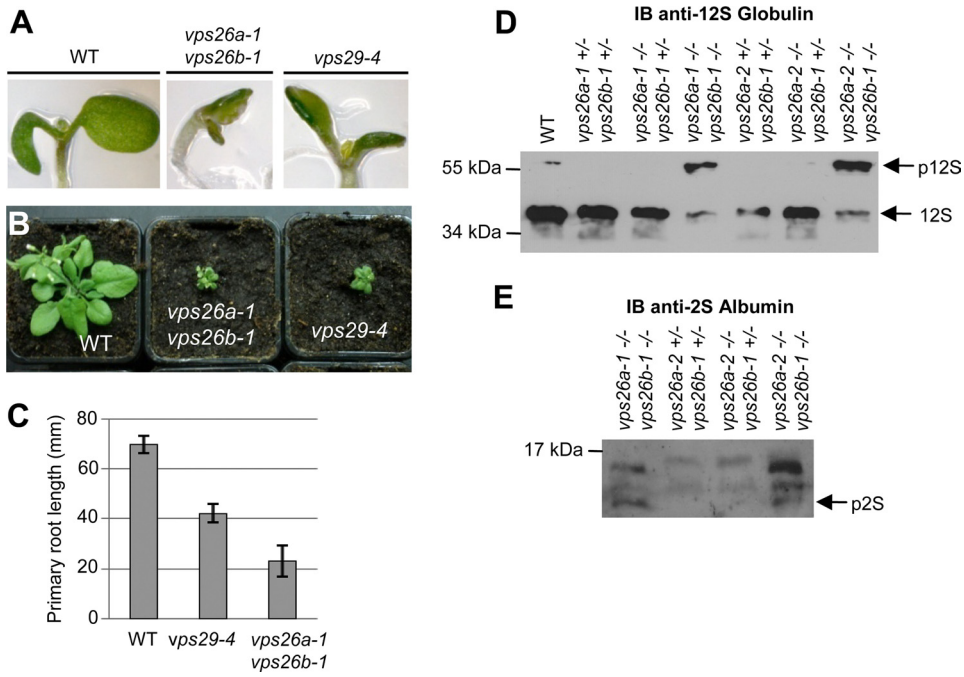

FIGURE 1. **vps26a vps26b double null mutants present defects similar to other *vps* mutants.** *A*, cotyledon phenotype of 7-day-old seedlings of *vps29-4* single and *vps26a-1 vps26b-1* double mutants compared with wild type (WT). *B*, phenotype of adult WT, *vps29-4* single, and *vps26a-1 vps26b-1* double mutant plants. *C*, measures of primary root length of 5-day-old seedlings from WT, *vps29-4* single, and *vps26a-1 vps26b-1* double mutant plants. Differences are significant with a p value < 0.001. *Error bars* show S.E. *D* and *E*, total protein extracts from WT and various combinations of *vps26a vps26b* mutant seeds were analyzed by Western blotting using anti-12S globulin and anti-2S albumin antibodies. *vps26a vps26b* homozygous double mutants present abnormal accumulation of precursors of 12S-globulin (p12S) (*D*) and 2S-albumin (p2S) (*E*). 12S, mature 12S-globulin. Molecular mass markers are indicated on the *left* in kDa.

VPS35, VPS26, and VPS29 had been previously identified *in vivo* (16), we failed to detect fluorescence in these BiFC assays as illustrated in Fig. 2*A* (*upper panel*) for VPS35/VPS26 interaction test. Previous studies in yeast and mammals reported that the depletion of a single core retromer member strongly affects the formation of the whole core retromer subcomplex (8, 10, 12, 13, 33–36). Thus, we repeated the BiFC experiment, but in addition to expressing the BiFC-tagged versions of VPS26a and VPS35a, we introduced the third VPS retromer member, VPS29, fused to mCherry, so as to reconstitute the *Arabidopsis* core retromer subcomplex in tobacco epidermal leaf cells. Under these conditions, where a proper stoichiometry of VPS retromer components is likely to be respected as the same promoter was used for driving protein expression, we observed fluorescence of the yellow fluorescent protein (YFP) resulting from VPS26a/VPS35a interaction (Fig. 2*A*, *lower panel*). This result suggests that the three VPS proteins are required simultaneously for the stability and correct assembly of the core retromer subcomplex in plant cells. Consistent with this assumption, VPS35a was previously described to be less abundant in the *Arabidopsis* weak *vps29-1/mag1-1* mutant (21). To assess whether the absence of SNXs or VPS retromer members could influence VPS35 accumulation, Western blot analysis using a specific anti-VPS35a antibody was performed on total protein extracts from various retromer-null mutants. Interestingly, we found that the decrease in VPS35a level was proportional to the strength of the *vps29* mutant allele, strong *vps29* alleles (*vps29-4*) leading to lower VPS35a accumulation than weaker ones (*vps29-1*) (Fig. 2*B*). In the absence of VPS26 isoforms, VPS35a was completely absent, as shown in Fig. 2*B*, whereas VPS29 accumulation was apparently not affected, although VPS29 was only recovered in the cytosolic fraction (see Fig. 4). Finally, complete depletion of the three SNX proteins did not affect VPS35a abundance, indicating that in *Arabidopsis*, as in mammals, the two retromer subcomplexes behave as biosynthetically independent units (10) (Fig. 2*B*). Hence, our data strongly support the idea that the stability of the core retromer is dependent on the stoichiometry of the three VPS components. However, in contrast to the mammalian and yeast retromer in which any VPS depletion leads to down-regulation of all other components, in plants, the retromer stability appears more subtly regulated with VPS26 playing a central role.

To go further in the study of plant retromer association with endosomal membranes and the involvement of the different VPS subunits in this mechanism, we decided to examine the cytosolic and microsomal distribution of endogenous VPS29 and VPS35a proteins in different *vps* mutant backgrounds. We focused on these two VPS proteins because specific antibodies were available for Western blotting detection. We found that, like in wild-type extracts, the distribution of VPS35a remained cytosolic and microsomal in *vps29*-null mutant (Fig. 3*A*) although, as expected, the amount of VPS35a was reduced in both fractions. These results indicate that VPS29 is not required for binding of VPS35a to membranes.

To determine to which membranes VPS35 is bound in *Arabidopsis* cells, we generated transgenic *Arabidopsis* plants stably expressing VPS35a fused to the green fluorescent protein (GFP) under the control of its own promoter, in a *vps29-4*$^{-/-}$-null mutant, in the *vps29-4*$^{+/-}$ heterozygous background that displays a wild-type phenotype and in *vps35a-1 vps35c-1* double mutants (supplemental Fig. 3*A*). VPS35a-GFP lines were first analyzed by Western blotting to check the proper expres-

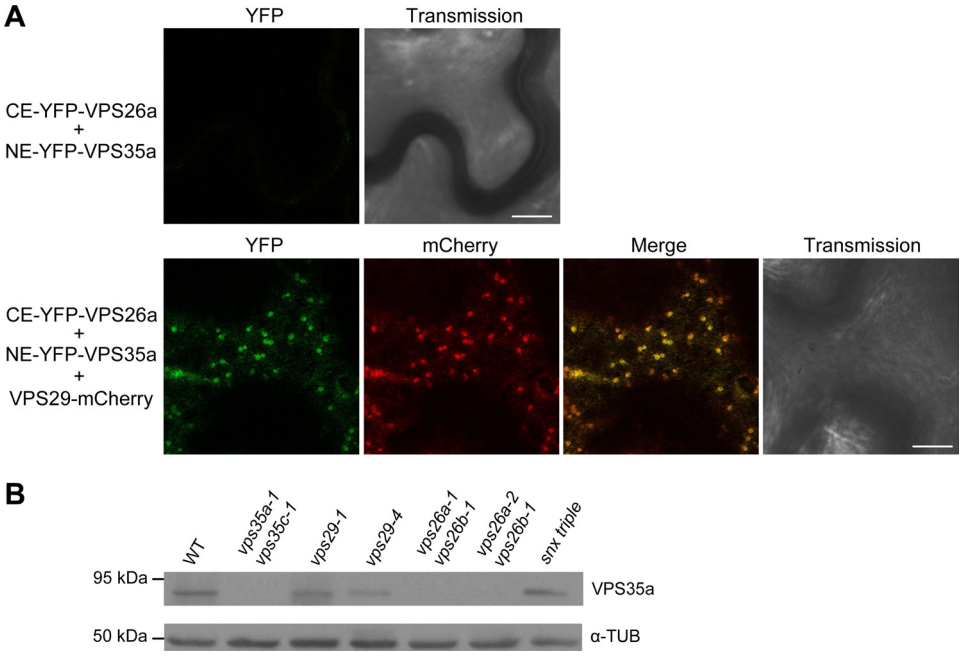

FIGURE 2. **Stability of the core retromer.** *A*, BiFC analysis of the interaction between NE-YFP-VPS35a and CE-YFP-VPS26a in epidermal cells of tobacco leaves in the absence (*upper panel*) or the presence of VPS29-mCherry (*lower panel*). In the absence of VPS29-mCherry, no interaction between VPS35a and VPS26a is detected. The YFP and mCherry channels, the superimposed image for the two channels (*Merge*), and images obtained with transmitted light (*transmission*) are shown. *Scale bars*, 10 μm. *B*, immunoblot analysis on total protein extracts from different *Arabidopsis* retromer mutants and wild-type (WT) plants using anti-VPS35a and anti-α-tubulin (α-*TUB*) antibodies. α-Tubulin was used as loading control. *snx triple* stands for *snx1-2 snx2a-2 snx2b-1*-null mutant. Molecular mass markers are indicated on the *left* in kDa.

sion of the fusion protein (supplemental Fig. 3*B*). The VPS35a-GFP protein was functional because it was capable of complementing the seed storage protein defects of *vps35a-1 vps35c-1* mutants (Fig. 3*B*) and its developmental defects (data not shown). In a *vps29-4*$^{+/-}$ background, VPS35a-GFP was found both in the cytosol and associated with punctate compartments (Fig. 3*C*). This was consistent with endosomal localization reported for SNXs, VPS29 and VPS35 in wild-type plants (16, 18, 20). In a *vps29-4*$^{-/-}$ background, VPS35a-GFP labeled punctate compartments as well as abnormally enlarged, vacuolated structures likely corresponding to aberrant endosomes (16) (Fig. 3*C*). These data support the results of our cell fractionation analysis and indicate that, in the absence of VPS29, VPS35a is still recruited to endosomal membranes. Unfortunately, we were unable to assess whether VPS26 was necessary for VPS35a membrane localization because of the dramatic decrease of this latter in *vps26a vps26b* double mutants (Fig. 2*B*). In these *vps26*-null mutants, VPS29 became completely soluble (Fig. 4), suggesting that VPS26 is required for VPS29 membrane recruitment. Although VPS26 was shown not to interact directly with VPS29 in a yeast two-hybrid assay (16), VPS26 might be necessary for the stability of the whole core retromer complex. However, because VPS35 protein is absent in *vps26a vps26b* mutants (Fig. 2*B*), we think that the lack of VPS35 rather than that of VPS26 is the cause of VPS29 release in the cytosol. Altogether, our results suggest that in plants VPS35 binds to membranes independently of VPS29 activity, whereas VPS29 requires the presence of both VPS26 and VPS35 to associate with the surface of endosomes.

VPS35 PRLYL Motif and C-end: Conserved Domains with Conserved Functions—Yeast and human VPS35 proteins contain a PRLYL motif in their N termini, which is directly involved in the interaction with VPS26 (11–13). This motif is conserved in *Arabidopsis* VPS35a and VPS35c, whereas VPS35b presents a substitution of the first leucine by methionine, resulting in the PRMYL motif. We investigated whether the interaction capacity of the PRLYL motif is conserved in *Arabidopsis* by generating two VPS35a mutants displaying point mutations in this motif. One, designated VPS35a-R104W (PWLYL), had arginine in position 104 substituted by tryptophan, and the other, VPS35a-L105P (PRPYL), had leucine in position 105 replaced by proline (supplemental Fig. 4*A*). Besides, in yeast and mammals, deletion of the C terminus of VPS35 affects the VPS35/VPS29 interaction (13, 37). Thus, we also generated a truncated form of VPS35a, designated VPS35a-ΔC-END (ΔC-END), in which the C terminus was deleted from the amino acid residue 647 (supplemental Fig. 4*A*). The capacity of these VPS35a mutated forms to bind VPS26 and VPS29 was tested in a yeast two-hybrid assay. Whereas wild-type VPS35a can bind both VPS26 isoforms and VPS29, the PWLYL and PRPYL mutant forms were unable to bind any of the other VPS subcomplex components (Fig. 5*A*). To confirm these results, we carried out a BiFC analysis in tobacco leaf epidermal cells that co-expressed VPS26a fused to the C-terminal half of YFP, the VPS29-mCherry protein, and either of the mutant forms of VPS35a fused to the N-terminal half of YFP. No YFP fluorescence was detected when we tested either the interaction between PWLYL and VPS26a or between PRPYL and VPS26a, indicating an absence of interaction (supplemental Fig. 4, *B* and *C*). Next, we looked at the role of the C-end of VPS35 in the interaction with VPS29. In the yeast two-hybrid assay, we found that ΔC-END still interacted with VPS26a and VPS26b but could not bind any more to VPS29 (Fig. 5*A*). Therefore, as in mammals, the PRLYL motif of *Arabidopsis* VPS35 is necessary for

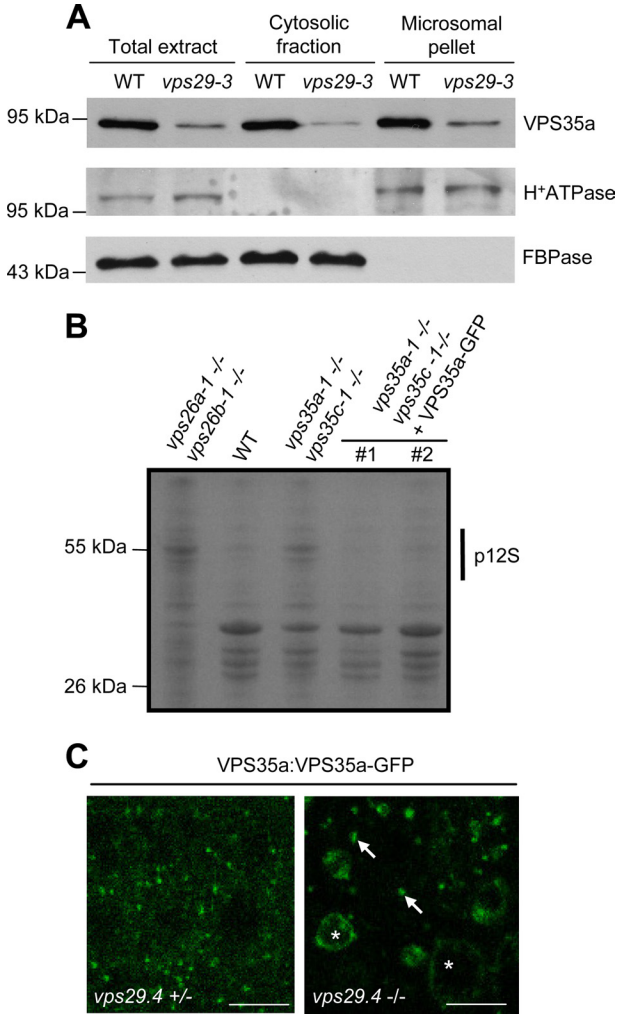

FIGURE 3. **VPS29 is dispensable for VPS35 membrane recruitment.** *A*, immunoblot analysis on total, cytosolic, and microsomal proteins from wild-type (WT) and *vps29-3* plantlets using anti-VPS35a, anti-H^+-ATPase, and anti-cytosolic FBPase antibodies. H^+-ATPase and FBPase were used as markers of membrane and cytosolic fractions, respectively. Molecular mass markers are indicated on the *left* in kDa. *B*, total proteins extracted from dry seeds of wild type (WT), *vps26a vps26b*, *vps35a vps35c*, and two transgenic *vps35a vps35c* independent lines (*#1* and *#2*) stably expressing the VPS35a-GFP fusion protein under the pVPS35a promoter. Extracts were analyzed by SDS-PAGE followed by Coomassie Blue staining of the gel. Transgenic lines exhibit a WT-like pattern of seed storage proteins compared with the mutants. p12S: precursor of 12S-globulin. Molecular mass markers are indicated on the *left* in kDa. *C*, confocal microscopy images illustrating the localization of VPS35a-GFP in the roots of *vps29-4*$^{+/-}$ (*left*) and *vps29*$-4^{-/-}$ (*right*) plants. *Arrows* indicate punctate compartments, and *asterisks* point to abnormally enlarged/vacuolated compartments labeled with VPS35a-GFP. *Scale bars*, 10 μm.

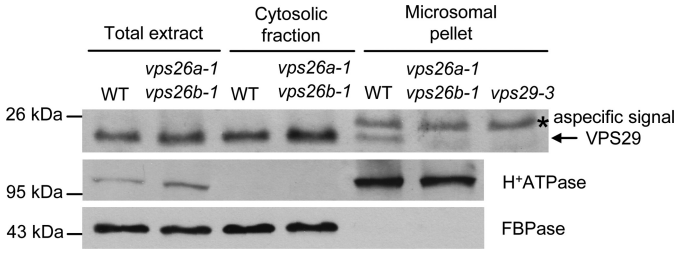

FIGURE 4. **VPS26 is required for VPS29 endosomal recruitment.** Immunoblot analysis of total, cytosolic, and microsomal proteins from wild-type (WT) and *vps26a-1 vps26b-1* plants using anti-VPS29, anti-H^+-ATPase, and anti-cytosolic FBPase antibodies. H^+-ATPase and FBPase were used as markers of membrane and cytosolic fractions, respectively. The *arrow* corresponds to VPS29, and the *asterisk* indicates a protein that is nonspecifically recognized by the anti-VPS29 antibody in microsomal fraction because it is detected in *vps29-3* mutant (*top panel*). Molecular mass markers are indicated on the *left* in kDa.

the association of VPS35 with VPS26, whereas its C terminus is required for the association with VPS29. It is worth noting that although the PWLYL and PRPYL mutant forms possess a proper C-terminal sequence, they are both unable to interact with VPS29 in a yeast two-hybrid assay. A similar result was already reported in yeast (13). This suggests that amino acid residues contained in the PRLYL motif and C terminus of VPS35 are required for the establishment of a stable interaction with VPS29.

VPS35 Can Interact with the Endosomal Membrane Independently of VPS26 and VPS29—In yeast and mammals, inhibition of the interaction between VPS35 and VPS26 results in the release in the cytosol of VPS35, indicating that VPS26 may be involved in VPS35 membrane recruitment (11). To determine whether *Arabidopsis* VPS26 may have a similar role, we compared the subcellular localization of wild-type VPS35a fused to GFP and transiently expressed in tobacco leaf cells with the localization of mutant and truncated forms of VPS35a. GFP-VPS35a protein was found dispersed in the cytosol or associated with punctate compartments, which likely correspond to endosomes (Fig. 5*B*). Interestingly, none of the mutated or truncated forms of VPS35a was altered in its localization, as they were found in the cytosol as well as associated with punctate structures (Fig. 5*B*). The distribution of wild-type and mutated/truncated VPS35a fusion proteins was further analyzed following cell fractionation and Western blotting using anti-GFP antibody. As shown in Fig. 5*C*, the distribution of VPS35a fusion proteins did not change when mutation/deletion that impaired their interactions with VPS26 or VPS29 proteins was introduced. These data indicate that *Arabidopsis* VPS35a can bind to membranes independently of other retromer components.

Core Retromer Assembly Can Occur in the Cytosol—Concerning the assembly of the core retromer, one hypothesis is that the complex may form first in the cytosol and then associates with the membrane of endosomes to fulfill its function in trafficking. To examine this possibility, we performed Co-IP experiments on cytosolic fractions obtained after cell fractionation of seedlings expressing VPS29-GFP fusion protein. Native immunoprecipitation (IP) was performed using an anti-GFP antibody, and the presence of the endogenous VPS35a in immunoprecipitates was assessed by Western blot analysis using an anti-VPS35a antibody. Plants expressing RABF2b and the a1 subunit of the vacuolar H^+-ATPase (VHA-a1) fused to GFP were used as negative controls, as both proteins localize to intracellular compartments, *i.e.* endosomes/prevacuolar compartment and the *trans*-Golgi network, respectively (23, 24, 38). The presence of VPS35a in immunoprecipitates containing VHA-a1-GFP or GFP-RABF2b was not detected, whereas VPS35a was strongly co-immunoprecipitated with VPS29-GFP (Fig. 6). These data are consistent with results of the BiFC assay (Fig. 2*A*), in which we observed that dimers of VPS35-VPS26 localized both to the cytosol and endosomal compartments. Altogether, these results demonstrate that the assembly of the core retromer can occur in the cytosol of plant cells.

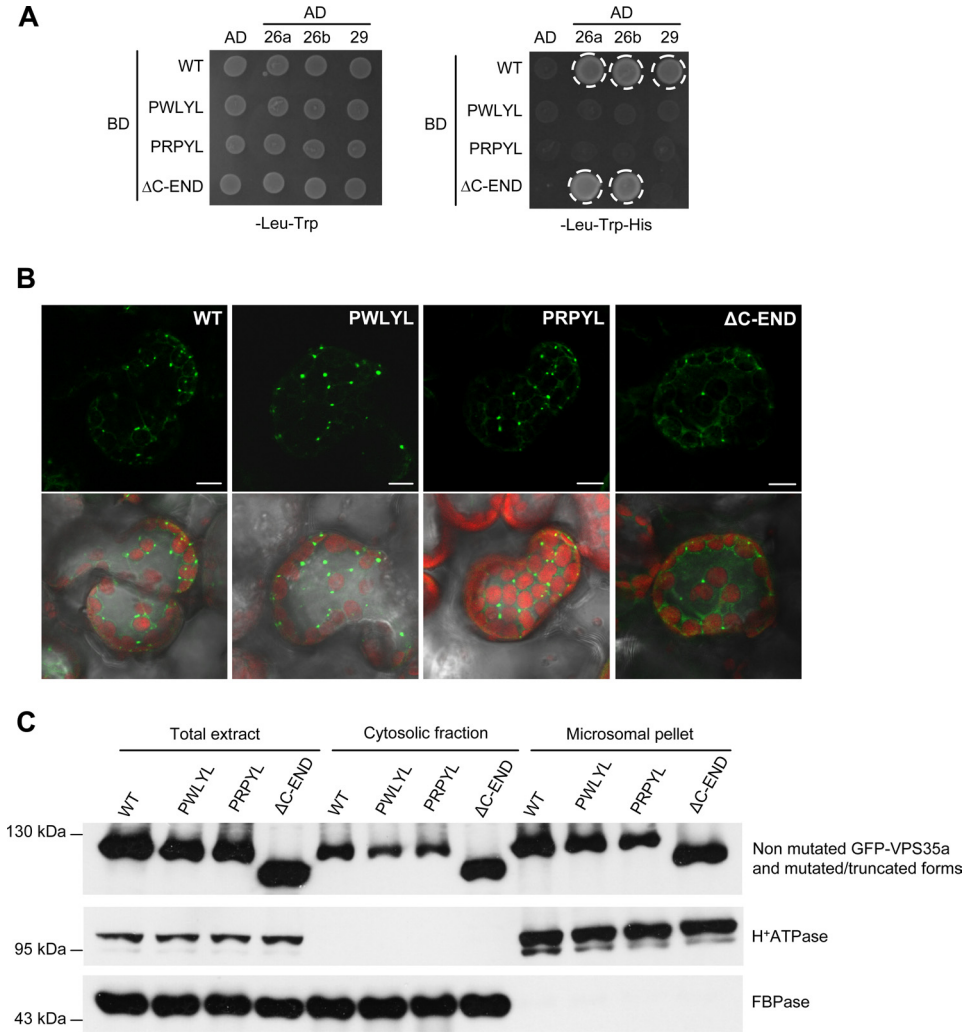

FIGURE 5. **VPS35 binds to membranes independently of VPS26 and VPS29.** *A*, yeast two-hybrid test monitoring the interaction between VPS26a, VPS26b, VPS29, and the wild-type (WT) and mutated/truncated forms of VPS35a. The corresponding empty vectors were used as negative controls. The interaction is revealed by the activation of *HIS3* transcription and growth on -His medium and is indicated by a white circle. The mutated VPS35a forms lose their capacity to bind to VPS26a, VPS26b, and VPS29, whereas the truncated VPS35a deleted of its C terminus can still associate with VPS26a and VPS26b, but not with VPS29. PWLYL, VPS35a-R104W; PRPYL, VPS35a-L105P; ΔC-END, VPS35a-ΔC-END; 26a, VPS26a; 26b, VPS26b; 29, VPS29; AD, Gal4 activation domain; BD, Gal4 binding domain. *B*, confocal microscopy analysis of the localization of WT, mutated (PWLYL, PRPYL), and C-terminal truncated (ΔC-END) forms of VPS35a tagged with GFP in *N. benthamiana* mesophyll leaf cells. Pictures below correspond to the overlay of GFP signals and images obtained with transmitted light. Chlorophyll autofluorescence in chloroplasts is seen in *red*. *Scale bars*, 10 μm. *C*, immunoblot analysis of total, cytosolic, and microsomal proteins extracted from tobacco leaves expressing GFP-tagged VPS35a or its mutated/truncated forms using anti-GFP, anti-H^+-ATPase, and anti-cytosolic FBPase antibodies. H^+-ATPase and FBPase were used as markers of membrane and cytosolic fractions, respectively. Molecular mass markers are indicated on the *left* in kDa. WT, wild-type VPS35a fused to GFP; PWLYL, GFP-VPS35a-R104W; PRPYL, GFP-VPS35a-L105P; ΔC-END, C-terminal truncated form of VPS35a fused to GFP.

Core Retromer Can interact with an Arabidopsis Rab7 Homolog on Endosomal Membranes—Studies relying on the structural analysis of the mammalian VPS subcomplex suggested that the core retromer cannot bind directly to lipids (39, 40). Indeed, the sequential action of two Rab GTPases, Rab5 and Rab7, regulates retromer recruitment to membranes in mammalian cells. First, Rab5, by promoting phosphatidylinositol 3-phosphate (PI3P) formation on endosomal membranes indirectly regulates the recruitment of SNXs to the endosomal surface, SNXs being essential for the proper localization of the core retromer (10, 14). Afterward, Rab7, in its active GTP-bound form, interacts with VPS35 and plays a major role in the recruitment of the core retromer to the membrane of endosomes (14, 15). To investigate whether *Arabidopsis* homologs of Rab7 might play a similar role in retromer recruitment, we looked for

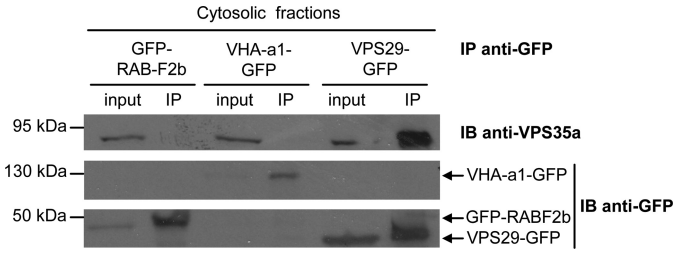

FIGURE 6. **VPS29 and VPS35 are able to associate in the cytosol.** Co-IP of VPS29-GFP and VPS35a was performed with an anti-GFP antibody on soluble fractions of transgenic plantlets expressing VPS29-GFP. Transgenic plantlets expressing either GFP-RabF2b or VHA-a1-GFP were used as negative controls for the IP assay. VPS35a and GFP-tagged proteins were detected with anti-VPS35a and anti-GFP antibodies, respectively. IB, immunoblotting. Molecular mass markers are indicated on the *left* in kDa.

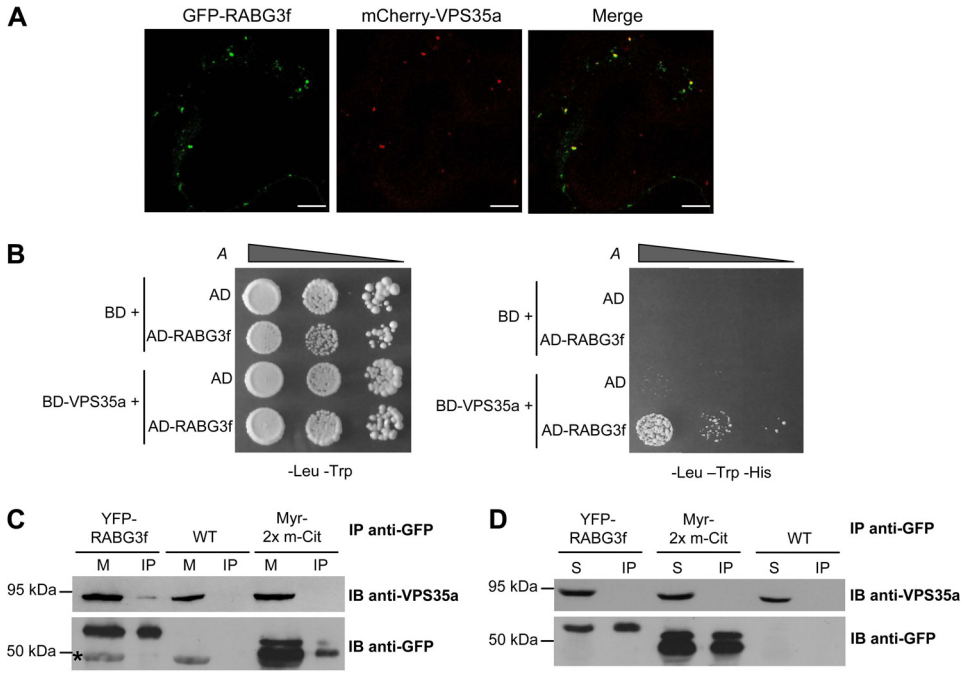

FIGURE 7. **VPS35a associates with RABG3f on membranes.** *A*, co-localization of mCherry-VPS35a with GFP-RABG3f in endosomal compartments. Confocal analysis was performed on epidermal cells of tobacco leaves co-expressing the two fusion proteins. *Scale bars*, 10 μm. *B*, yeast two-hybrid test monitoring the interaction between VPS35a and RABG3f. The corresponding empty vectors were used as negative controls. Yeast transformants were grown in liquid cultures and diluted to $A_{600\ nm} = 0.2$, 0.02, and 0.002 and then spotted on −Leu −Trp (*left panel*) and −Leu −Trp −His (*right panel*) synthetic complete (SC) medium. The interaction is revealed by the activation of *HIS3* transcription and growth on −His medium. AD, Gal4 activation domain; BD, Gal4 DNA binding domain. *C*, co-IP of YFP-RABG3f and VPS35a with an anti-GFP antibody from microsomal protein extracts of transgenic plantlets expressing YFP-RABG3f. Transgenic plantlets expressing the partially membrane localized protein 2× mCitrine containing a myristoylation tail (Myr-2× m-Cit), as well as wild-type (WT) plantlets were used to test the specificity of the YFP-RABG3f/VPS35a interaction. VPS35a and GFP-tagged proteins were detected with anti-VPS35a and anti-GFP antibodies, respectively. The *asterisk* indicates a protein that is nonspecifically recognized by the anti-GFP antibody in microsomal fraction. M, microsomal pellet (Input); IP, immunoprecipitate; IB, immunoblotting. *D*, immunoprecipitation (IP) assays from cytosolic fractions of YFP-RABG3f and Myr-2× m-Cit transgenic and WT plants reveal that VPS35a does not interact with YFP-RABG3f in the soluble fraction. IP and immunodetection were conducted as in *C*. S, soluble fractions (Input).

possible physical interactions between these proteins and VPS35. In the *Arabidopsis* genome, there are six genes coding for Rab7 homologs, which form the *RABG3* subclass with isoforms *RABG3a* to *RABG3f* (41, 42). We decided to focus our analysis on RABG3f protein because this isoform displays the highest percentage of identity with mammalian Rab7 (68% identity with human Rab7). First, we showed by transiently co-expressing GFP-RABG3f and mCherry-VPS35a in tobacco leaf cells that the two proteins co-localized in punctate compartments that likely correspond to endosomes (Fig. 7*A*). Next, we showed that RABG3f and VPS35a physically and directly interact in yeast two-hybrid assays (Fig. 7*B*). To confirm this interaction *in planta*, we used transgenic *Arabidopsis* plants expressing YFP-RABG3f (25) and carried out co-immunoprecipitation experiments on microsomal and cytosolic fractions using an anti-GFP antibody. The presence of the endogenous VPS35a in immunoprecipitates was assessed by Western blot analysis using an anti-VPS35a antibody. As negative controls, we used fractions prepared from wild-type or transgenic plants overexpressing a 2× mCitrine tag containing a myristoylation tail (Myr-2× m-Cit), which allows partial membrane anchoring of this fusion protein (26). We detected the presence of the endogenous VPS35a in immunoprecipitates obtained from microsomal fractions of YFP-RABG3f lines, but not of Myr-2× m-Cit or wild-type plants (Fig. 7*C*). Interestingly VPS35a was not found in immunoprecipitates obtained from cytosolic fractions of YFP-RABG3f plants (Fig. 7*D*). Thus, it appears that the interaction between VPS35a and RABG3f occurs *in planta* only in the membrane fraction where the GTPase is supposed to be in its active GTP-bound form.

DISCUSSION

Phenotypes of Retromer Mutants Depend on the Relative Abundance of VPS35 Protein—In this study, by analyzing null mutants for VPS26 isoforms, we showed that VPS26 proteins function together with VPS29 in mediating *Arabidopsis* developmental processes (Fig. 1). Interestingly, we found an aggravation of the root phenotype in *vps26a vps26b* double mutants compared with the *vps29* mutant. It appears that the strength of the phenotypes of retromer mutants is correlated with the amounts of VPS35 protein present in mutant seedlings. Indeed, in *vps26a vps26b* mutants, VPS35a is completely absent, whereas in *vps29* only a partial decrease in VPS35a level is observed. Moreover, weak alleles of *vps29* are less affected than the strong ones regarding the decrease in VPS35a amount (Fig. 2*B*). These results support the hypothesis of VPS35 playing a central role in the assembly and function of the retromer complex. In agreement with this idea, the *vps35a vps35b vps35c* triple mutant was reported to be lethal (19).

Core Retromer Associates with Endosomal Membranes Where It Interacts with RABG3f—Unlike the animal retromer, we have previously demonstrated that *Arabidopsis* SNX pro-

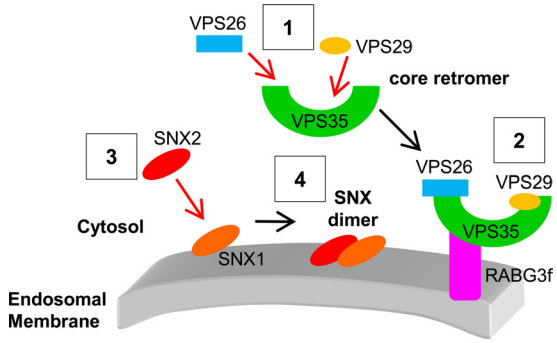

FIGURE 8. **Tentative model of the assembly of the core retromer to endosomal membranes in plants.** The core retromer assembles first in the cytosol (*1*) and then is recruited to the endosomal membrane through an interaction between VPS35 and RABG3f (*2*). This recruitment occurs independently of SNX proteins. SNXs participate in certain functions of the core retromer through the formation of membrane-bound heterodimers consisting of SNX1 and SNX2s. In plants, SNX1 is the only SNX capable of binding to the membrane of endosomes (*3*) and will recruit cytosolic SNX2s to form a functional SNX complex (*4*).

teins are not required for association of the core retromer with membranes (20). Our work reveals that among VPS retromer components, VPS35 is necessary and sufficient for the membrane recruitment of the core retromer. Indeed, in the absence of VPS29, VPS35 can still reach endosomes (Fig. 3) and similarly, VPS35-ΔC-END, a truncated form of VPS35 that cannot bind VPS29, is properly localized to the cytosol and endosomes in plant cells (Fig. 5). The absence of VPS26 strongly affects the distribution of VPS29, which is released in the cytosol (Fig. 4), although a direct interaction between VPS26 and VPS29 has never been established (16). Considering our observation that VPS35 is completely absent when VPS26 is missing, we may assume that the dissociation of VPS29 from membranes in *vps26*-null mutants is caused by the absence of VPS35. Finally, when VPS35 is mutated in regions important for binding to VPS26, the mutated VPS35 forms are still associated with membranes, suggesting again that VPS35 is the main component responsible for the core retromer recruitment to the endosomal membrane in *Arabidopsis*. Based on our observations, we propose a model in which the core retromer assembles in the cytosol (Fig. 6), with VPS35 directly binding to VPS26 and VPS29. Then, the VPS subcomplex is recruited to membranes through VPS35, independently of the activity of SNXs (Fig. 8). Our results reveal a distinct mode of assembly of the core retromer in plant cells, compared with yeast and mammalian cells. In these latter, it has been reported that mutated forms of VPS35 that are unable to interact with VPS26 are released in the cytosol (11), giving an essential role for VPS26 in the recruitment of the core retromer to membranes. Our work also provides evidence that in plants VPS35 can form a complex with the Rab7 homolog RABG3f (Fig. 7), highlighting that VPS35-Rab7 interaction is a conserved mechanism in yeast (43), mammals (14, 15), and plants. Based on our results and the yeast and mammal literature, we speculate that plant RABG3f, when active, associates with membranes and binds to VPS35, hence participating in the recruitment of the core retromer to the surface of endosomes (Fig. 8). Interestingly, in previous studies performed in mammals, some authors hypothesized that in addition to the association with Rab7, interaction with transmembrane cargo proteins may help to stabilize the endosomal membrane recruitment of the core retromer (14, 15). Such a scenario might also occur in plants.

One or More Retromer Complexes in Plants?—As *VPS26* and *VPS35* are multicopy genes in *Arabidopsis*, we can question whether several retromer complexes exist in plants. In mammals, the existence of four retromer complexes has recently been proposed, depending on the pair of SNXs that associates within the complex (4). Considering the results of our IP and yeast two-hybrid experiments, all *Arabidopsis* isoforms of VPS35 are capable of binding both VPS26a and VPS26b, as well as VPS29 (16). In addition, impairing the function of a single VPS26 or VPS35 isoform does not lead to any apparent phenotype, suggesting that the isoforms are redundant and presumably interchangeable within the retromer complex (Ref. 19 and this work). Recently, *vps35a* was found in a genetic screen performed to isolate mutants able to suppress the phenotype of *zig-1*, a mutant affected in shoot gravitropism and morphology. However, neither *vps35b* nor *vps35c* mutants were able to affect the *zig-1* phenotype (44). Similarly, *VPS26a* and *VPS26b* genes presented distinct functions regarding their ability to suppress the phenotype of *zig-1* (44). We recently reported that *SNX2a* and *SNX2b*, which seem to act redundantly because single mutants do not present abnormalities in their development, have however separate functions in a *vps29* background (20). Overall, these genetic analyses reveal the existence of overlapping as well as distinct functions for retromer isoforms. The existence of different combinations of retromer complexes remains an open question, and it would be interesting to examine in more detail whether some VPS bind preferentially to other isoforms, as well as whether specific isoform associations may occur in particular tissues, developmental stages, or environmental conditions.

To conclude, we have now accumulated evidence that the plant retromer complex controls a wide range of developmental processes. Although its mechanism of action is still poorly understood, in the present work we shed light on how the core retromer assembles and is recruited to the endosomal membranes. We also reveal that the plant retromer exhibits original and unexpected features compared with its animal and yeast counterparts. The main challenge for the future remains to identify cargoes that are sorted by the core retromer, as well as understand better the functional interactions that may occur between the SNX and VPS subcomplexes.

Acknowledgments—We thank Dr. I. Hara-Nishimura for the anti-VPS35a, anti-12S globulin, and anti-2S albumin antibodies and for vps35a-1 vps35c-1 and vps29–1 seeds; Professor Marc Boutry for the anti-H^+-ATPase antibodies; Dr. K. Schumacher for the VHA-a1: VHA-a1-GFP line; Dr. F. Parcy for the pBIFP vectors; and Dr. M. Vidal for the pPC97 and pPC86CYH2S vectors. We thank C. Lionnet and C. Chamot from the Institut Fédératif de Recherche (IFR) 128 and the Plateau Technique d'Imagerie/Microscopie (PLATIM) for technical assistance in confocal microscopy; Dr. A. Chaboud for help with yeast two-hybrid assays; and A. Lacroix, P. Angelot, Y. Rasmus, and I. Desbouchages for plant care. We thank the Max Planck Institute and the SALK Institute for the insertion mutant lines, and the Nottingham Arabidopsis Stock Centre for YFP-RABG3f.

REFERENCES

1. Attar, N., and Cullen, P. J. (2010) The retromer complex. *Adv. Enzyme Regul.* **50,** 216–236
2. Griffin, C. T., Trejo, J., and Magnuson, T. (2005) Genetic evidence for a mammalian retromer complex containing sorting nexins 1 and 2. *Proc. Natl. Acad. Sci. U.S.A.* **102,** 15173–15177
3. Wassmer, T., Attar, N., Bujny, M. V., Oakley, J., Traer, C. J., and Cullen, P. J. (2007) A loss-of-function screen reveals SNX5 and SNX6 as potential components of the mammalian retromer. *J. Cell Sci.* **120,** 45–54
4. Wassmer, T., Attar, N., Harterink, M., van Weering, J. R., Traer, C. J., Oakley, J., Goud, B., Stephens, D. J., Verkade, P., Korswagen, H. C., and Cullen, P. J. (2009) The retromer coat complex coordinates endosomal sorting and dynein-mediated transport, with carrier recognition by the trans-Golgi network. *Dev. Cell* **17,** 110–122
5. Nothwehr, S. F., Bruinsma, P., and Strawn, L. A. (1999) Distinct domains within Vps35p mediate the retrieval of two different cargo proteins from the yeast prevacuolar/endosomal compartment. *Mol. Biol. Cell* **10,** 875–890
6. Nothwehr, S. F., Ha, S. A., and Bruinsma, P. (2000) Sorting of yeast membrane proteins into an endosome-to-Golgi pathway involves direct interaction of their cytosolic domains with Vps35p. *J. Cell Biol.* **151,** 297–310
7. Seaman, M. N. (2007) Identification of a novel conserved sorting motif required for retromer-mediated endosome-to-TGN retrieval. *J. Cell Sci.* **120,** 2378–2389
8. Arighi, C. N., Hartnell, L. M., Aguilar, R. C., Haft, C. R., and Bonifacino, J. S. (2004) Role of the mammalian retromer in sorting of the cation-independent mannose 6-phosphate receptor. *J. Cell Biol.* **165,** 123–133
9. Tabuchi, M., Yanatori, I., Kawai, Y., and Kishi, F. (2010) Retromer-mediated direct sorting is required for proper endosomal recycling of the mammalian iron transporter DMT1. *J. Cell Sci.* **123,** 756–766
10. Rojas, R., Kametaka, S., Haft, C. R., and Bonifacino, J. S. (2007) Interchangeable but essential functions of SNX1 and SNX2 in the association of retromer with endosomes and the trafficking of mannose 6-phosphate receptors. *Mol. Cell Biol.* **27,** 1112–1124
11. Gokool, S., Tattersall, D., Reddy, J. V., and Seaman, M. N. (2007) Identification of a conserved motif required for Vps35p/Vps26p interaction and assembly of the retromer complex. *Biochem. J.* **408,** 287–295
12. Zhao, X., Nothwehr, S., Lara-Lemus, R., Zhang, B. Y., Peter, H., and Arvan, P. (2007) Dominant negative behavior of mammalian Vps35 in yeast requires a conserved PRLYL motif involved in retromer assembly. *Traffic* **8,** 1829–1840
13. Restrepo, R., Zhao, X., Peter, H., Zhang, B. Y., Arvan, P., and Nothwehr, S. F. (2007) Structural features of vps35p involved in interaction with other subunits of the retromer complex. *Traffic* **8,** 1841–1853
14. Rojas, R., van Vlijmen, T., Mardones, G. A., Prabhu, Y., Rojas, A. L., Mohammed, S., Heck, A. J., Raposo, G., van der Sluijs, P., and Bonifacino, J. S. (2008) Regulation of retromer recruitment to endosomes by sequential action of Rab5 and Rab7. *J. Cell Biol.* **183,** 513–526
15. Seaman, M. N., Harbour, M. E., Tattersall, D., Read, E., and Bright, N. (2009) Membrane recruitment of the cargo-selective retromer subcomplex is catalysed by the small GTPase Rab7 and inhibited by the Rab-GAP TBC1D5. *J. Cell Sci.* **122,** 2371–2382
16. Jaillais, Y., Santambrogio, M., Rozier, F., Fobis-Loisy, I., Miège, C., and Gaude, T. (2007) The retromer protein VPS29 links cell polarity and organ initiation in plants. *Cell* **130,** 1057–1070
17. Vanoosthuyse, V., Tichtinsky, G., Dumas, C., Gaude, T., and Cock, J. M. (2003) Interaction of calmodulin, a sorting nexin and kinase-associated protein phosphatase with the *Brassica oleracea* S locus receptor kinase. *Plant Physiol.* **133,** 919–929
18. Oliviusson, P., Heinzerling, O., Hillmer, S., Hinz, G., Tse, Y. C., Jiang, L., and Robinson, D. G. (2006) Plant retromer, localized to the prevacuolar compartment and microvesicles in *Arabidopsis*, may interact with vacuolar sorting receptors. *Plant Cell* **18,** 1239–1252
19. Yamazaki, M., Shimada, T., Takahashi, H., Tamura, K., Kondo, M., Nishimura, M., and Hara-Nishimura, I. (2008) *Arabidopsis* VPS35, a retromer component, is required for vacuolar protein sorting and involved in plant growth and leaf senescence. *Plant Cell Physiol.* **49,** 142–156
20. Pourcher, M., Santambrogio, M., Thazar, N., Thierry, A. M., Fobis-Loisy, I., Miège, C., Jaillais, Y., and Gaude, T. (2010) Analyses of sorting nexins reveal distinct retromer-subcomplex functions in development and protein sorting in *Arabidopsis thaliana*. *Plant Cell* **22,** 3980–3991
21. Shimada, T., Koumoto, Y., Li, L., Yamazaki, M., Kondo, M., Nishimura, M., and Hara-Nishimura, I. (2006) AtVPS29, a putative component of a retromer complex, is required for the efficient sorting of seed storage proteins. *Plant Cell Physiol.* **47,** 1187–1194
22. Alonso, J. M., Stepanova, A. N., Leisse, T. J., Kim, C. J., Chen, H., Shinn, P., Stevenson, D. K., Zimmerman, J., Barajas, P., Cheuk, R., Gadrinab, C., Heller, C., Jeske, A., Koesema, E., Meyers, C. C., Parker, H., Prednis, L., Ansari, Y., Choy, N., Deen, H., Geralt, M., Hazari, N., Hom, E., Karnes, M., Mulholland, C., Ndubaku, R., Schmidt, I., Guzman, P., Aguilar-Henonin, L., Schmid, M., Weigel, D., Carter, D. E., Marchand, T., Risseeuw, E., Brogden, D., Zeko, A., Crosby, W. L., Berry, C. C., and Ecker, J. R. (2003) Genome-wide insertional mutagenesis of *Arabidopsis thaliana*. *Science* **301,** 653–657
23. Jaillais, Y., Fobis-Loisy, I., Miège, C., Rollin, C., and Gaude, T. (2006) AtSNX1 defines an endosome for auxin-carrier trafficking in *Arabidopsis*. *Nature* **443,** 106–109
24. Dettmer, J., Hong-Hermesdorf, A., Stierhof, Y. D., and Schumacher, K. (2006) Vacuolar H^+-ATPase activity is required for endocytic and secretory trafficking in *Arabidopsis*. *Plant Cell* **18,** 715–730
25. Geldner, N., Dénervaud-Tendon, V., Hyman, D. L., Mayer, U., Stierhof, Y. D., and Chory, J. (2009) Rapid, combinatorial analysis of membrane compartments in intact plants with a multicolor marker set. *Plant J.* **59,** 169–178
26. Jaillais, Y., Hothorn, M., Belkhadir, Y., Dabi, T., Nimchuk, Z. L., Meyerowitz, E. M., and Chory, J. (2011) Tyrosine phosphorylation controls brassinosteroid receptor activation by triggering membrane release of its kinase inhibitor. *Genes Dev.* **25,** 232–237
27. Fobis-Loisy, I., Chambrier, P., and Gaude, T. (2007) Genetic transformation of *Arabidopsis lyrata*: specific expression of the green fluorescent protein (GFP) in pistil tissues. *Plant Cell Rep.* **26,** 745–753
28. Karimi, M., De Meyer, B., and Hilson, P. (2005) Modular cloning in plant cells. *Trends Plant Sci.* **10,** 103–105
29. Karimi, M., Inzé, D., and Depicker, A. (2002) GATEWAY vectors for *Agrobacterium*-mediated plant transformation. *Trends Plant Sci.* **7,** 193–195
30. Desprez, T., Juraniec, M., Crowell, E. F., Jouy, H., Pochylova, Z., Parcy, F., Höfte, H., Gonneau, M., and Vernhettes, S. (2007) Organization of cellulose synthase complexes involved in primary cell wall synthesis in *Arabidopsis thaliana*. *Proc. Natl. Acad. Sci. U.S.A.* **104,** 15572–15577
31. Shimada, T., Fuji, K., Tamura, K., Kondo, M., Nishimura, M., and Hara-Nishimura, I. (2003) Vacuolar sorting receptor for seed storage proteins in *Arabidopsis thaliana*. *Proc. Natl. Acad. Sci. U.S.A.* **100,** 16095–16100
32. Morsomme, P., Dambly, S., Maudoux, O., and Boutry, M. (1998) Single point mutations distributed in 10 soluble and membrane regions of the *Nicotiana plumbaginifolia* plasma membrane PMA2 H^+-ATPase activate the enzyme and modify the structure of the C-terminal region. *J. Biol. Chem.* **273,** 34837–34842
33. Seaman, M. N. (2004) Cargo-selective endosomal sorting for retrieval to the Golgi requires retromer. *J. Cell Biol.* **165,** 111–122
34. Vergés, M., Luton, F., Gruber, C., Tiemann, F., Reinders, L. G., Huang, L., Burlingame, A. L., Haft, C. R., and Mostov, K. E. (2004) The mammalian retromer regulates transcytosis of the polymeric immunoglobulin receptor. *Nat. Cell Biol.* **6,** 763–769
35. Reddy, J. V., and Seaman, M. N. (2001) Vps26p, a component of retromer, directs the interactions of Vps35p in endosome-to-Golgi retrieval. *Mol. Biol. Cell* **12,** 3242–3256
36. Seaman, M. N., McCaffery, J. M., and Emr, S. D. (1998) A membrane coat complex essential for endosome-to-Golgi retrograde transport in yeast. *J. Cell Biol.* **142,** 665–681
37. Hierro, A., Rojas, A. L., Rojas, R., Murthy, N., Effantin, G., Kajava, A. V., Steven, A. C., Bonifacino, J. S., and Hurley, J. H. (2007) Functional architecture of the retromer cargo-recognition complex. *Nature* **449,** 1063–1067
38. Jaillais, Y., Fobis-Loisy, I., Miège, C., and Gaude, T. (2008) Evidence for a

sorting endosome in Arabidopsis root cells. *Plant J.* **53,** 237–247
39. Collins, B. M., Skinner, C. F., Watson, P. J., Seaman, M. N., and Owen, D. J. (2005) Vps29 has a phosphoesterase fold that acts as a protein interaction scaffold for retromer assembly. *Nat. Struct. Mol. Biol.* **12,** 594–602
40. Shi, H., Rojas, R., Bonifacino, J. S., and Hurley, J. H. (2006) The retromer subunit Vps26 has an arrestin fold and binds Vps35 through its C-terminal domain. *Nat. Struct. Mol. Biol.* **13,** 540–548
41. Rutherford, S., and Moore, I. (2002) The *Arabidopsis* Rab GTPase family: another enigma variation. *Curr. Opin. Plant Biol.* **5,** 518–528
42. Woollard, A. A., and Moore, I. (2008) The functions of Rab GTPases in plant membrane traffic. *Curr. Opin. Plant Biol.* **11,** 610–619
43. Liu, T. T., Gomez, T. S., Sackey, B. K., Billadeau, D. D., and Burd, C. G. (2012) Rab GTPase regulation of retromer-mediated cargo export during endosome maturation. *Mol. Biol. Cell* **23,** 2505–2515
44. Hashiguchi, Y., Niihama, M., Takahashi, T., Saito, C., Nakano, A., Tasaka, M., and Morita, M. T. (2010) Loss-of-function mutations of retromer large subunit genes suppress the phenotype of an *Arabidopsis zig* mutant that lacks Qb-SNARE VTI11. *Plant Cell* **22,** 159–172

Mechanisms Governing the Endosomal Membrane Recruitment of the Core Retromer in *Arabidopsis*

Enric Zelazny, Martina Santambrogio, Mikael Pourcher, Pierre Chambrier, Annick Berne-Dedieu, Isabelle Fobis-Loisy, Christine Miège, Yvon Jaillais and Thierry Gaude

J. Biol. Chem. 2013, 288:8815-8825.
doi: 10.1074/jbc.M112.440503 originally published online January 29, 2013